Itinerant chimeras in an adaptive network of pulse-coupled oscillators

Dmitry V. Kasatkin, Vladimir V. Klinshov, and Vladimir I. Nekorkin
Institute of Applied Physics of the Russian Academy of Sciences, 46 Ul'yanov Street, 603950, Nizhny Novgorod, Russia

(Received 13 September 2018; revised manuscript received 5 December 2018; published 7 February 2019)

In a network of pulse-coupled oscillators with adaptive coupling, we discover a dynamical regime which we call an "itinerant chimera." Similarly as in classical chimera states, the network splits into two domains, the coherent and the incoherent. The drastic difference is that the composition of the domains is volatile, i.e., the oscillators demonstrate spontaneous switching between the domains. This process can be seen as traveling of the oscillators from one domain to another or as traveling of the chimera core across the network. We explore the basic features of the itinerant chimeras, such as the mean and the variance of the core size, and the oscillators lifetime within the core. We also study the scaling behavior of the system and show that the observed regime is not a finite-size effect but a key feature of the collective dynamics which persists even in large networks.

DOI: 10.1103/PhysRevE.99.022203

I. INTRODUCTION

Networks of interacting nodes are omnipresent in nature and technology [1]. In recent decades, a specific type of collective behavior called "chimera states" is intensively explored in networks of coupled oscillators. Chimera states manifest themselves as spontaneous symmetry breaking in systems of identical and symmetrically coupled oscillators which split into phase-coherent and phase-incoherent parts. First observed by Kuramoto and Battogtokh [2] and later named "chimeras" by Abrams and Strogatz [3], this type of partial synchronization later attracted much attention of specialists in dynamical networks. Chimera states were discovered and studied for networks of various configurations, and experimental observations were provided as well (see the reviews [4,5] and references therein).

The analytical study of the chimera states was carried out in the continuum limit, see, for example, Refs. [6–8]. However, for the finite network size the rigorous analysis is hardly possible, and the results rely on the intensive numerical studies. It was shown that finite-size effects have a pronounced influence on the chimera states. In particular, the lifetime of chimeras quickly decreases as the number of oscillators in the network becomes smaller [9]. Another characteristic feature is the Brownian-like motion of the chimera position, i.e., location of the coherent domain in the network [10]. The effective diffusion coefficient quickly drops as the network size grows which allows to associate the motion to finite-size effects.

In the present paper, we demonstrate a new type of chimera-like behavior which we call an "itinerant chimera." Similarly, with classical chimeras, in this state the network splits into the coherent and the incoherent domains. However, the drastic difference is the volatile composition of the domains. As the time passes, each oscillator demonstrates spontaneous transitions between the domains, so that none of them remains in the same domain forever. From the collective dynamics viewpoint, this process can be seen as the traveling of the synchronized core across the network. Importantly, the core motion is not just a finite-size effect observed for small number of interacting units but rather a key characteristic of the network dynamics which persists even for large networks.

The motion of the chimera's core was reported in a number of previous works. In Ref. [10] it was shown that Brownian-like motion is intrinsic for chimeras, but the effective diffusion coefficient vanishes for large networks. The disrupted chimera ordering with the wandering incoherent domain was observed in a lattice of spins [11]. In Ref. [12] the so-called resurgence of chimera states was reported which manifests itself as spontaneous emergence of chimeras at random positions where they exist for some time and later disappear. Transient chimeras in modular networks were observed in Ref. [13] where the synchrony in different modules was rising and falling in irregular manner. Alternating chimeras were observed where the coherent and incoherent domains swapped on course of the network dynamics [14,15]. In Ref. [16] hetoroclinic switching between chimeras was demonstrated which can be interpreted as periodical traveling of the chimera across the network. The most typical type of chimera motion is a constant-speed drift which may be induced by such factors as the sign-alternating coupling function [17], coupling asymmetry [18,19], nonlinear coupling [20], or coupling delay [21]. This drift may be used in control schemes for stabilization of the chimera's position [22–24]. The drastic difference of our model is that the core motion is randomlike, but it does not vanish as the network size grows. Therefore we consider itinerant chimeras reported herein as a novel dynamical regime observed for the first time.

II. MODEL

Our model is a network of phase oscillators with pulse coupling. The pulse coupling scheme was used in order to speed up the numerical simulations by using the effective reduction schemes [25]. On the other hand, pulse-coupled oscillators are often seen as a conceptual model for populations of neurons. In the phase oscillator representation, neurons are characterized by their phase response functions (PRCs) which may be calculated for any neuronal model [26,27].

 ©2019 American Physical Society

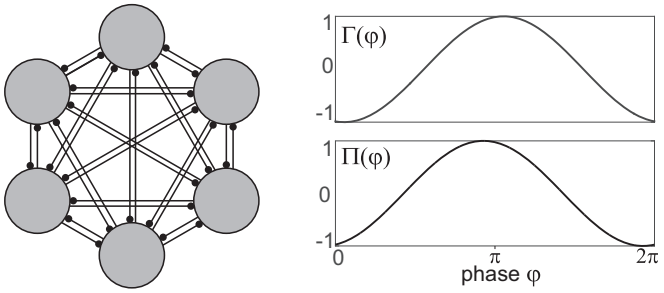

FIG. 1. Left: The circuitry of the studied network. Large gray circles denote oscillators, black lines denote all-to-all coupling, and small black circles stand for adaptive coupling strength. Right: The plots of the PRC $\Gamma(\varphi) = -\sin(\varphi + \alpha)$ and the adaptivity function $\Pi(\varphi) = \sin(\varphi + \beta)$ for the standard parameter values $\alpha = 1.4$ and $\beta = 4.94$.

A distinctive feature of our model is that the coupling weights are not constant but rather evolve according to a certain plasticity rule. In the context of neuronal networks, the coupling weights evolution corresponds to various plasticity mechanisms which change the strength of the synapses. Recent studies have demonstrated the importance of the timing of individual spikes in synaptic plasticity [28–30]. In order to account for such spike-timing-dependent plasticity (STDP) in our model the dynamics of the coupling weights is phase dependent.

Our network of N identical all-to-all coupled oscillators is given by the system

$$\frac{d\varphi_j}{dt} = \omega + \frac{1}{N}\sum_{k\neq j}\kappa_{jk}\Gamma(\varphi_j)\sum_{t_k}\delta(t - t_k), \tag{1}$$

$$\frac{d\kappa_{jk}}{dt} = \varepsilon\left[-\kappa_{jk} + \Pi(\varphi_j)\sum_{t_k}\delta(t - t_k)\right]. \tag{2}$$

Here $\varphi_j \in [0; 2\pi]$ is the jth oscillator's phase, κ_{jk} is the strength of the connection from the kth to jth oscillator [31], $\Gamma(\varphi)$ is the phase response curve, ε is a (small) parameter controlling the adaptation rate, while function $\Pi(\varphi)$ defines the plasticity rule (see Fig. 1). In the absence of coupling, each oscillator has the same native frequency $\omega = 1$, and its phase grows uniformly. When the phase reaches 2π, it resets to zero, and the oscillator emits a pulse. The coupling is pulselike and described by the double sum in (1). The first sum runs over all oscillators $k \neq j$, while the second sum runs over all moments t_k when the kth oscillator produces pulses. Each pulse is instantly received by the jth oscillator and causes the latter's momentary phase shift $\Delta\varphi_j = \kappa_{jk}\Gamma(\varphi_j)$. We take the phase response curve in the form $\Gamma(\varphi) = -\sin(\varphi + \alpha)$, where α is the coupling phase lag.

In the absence of pulses, the coupling coefficients κ_{jk} relax to zero with the rate defined by ε. Each pulse produced by oscillator k leads to momentary change of its connections to all other oscillators so that κ_{jk} changes by $\Delta\kappa_{jk} = \Pi(\varphi_j)$. The plasticity rule is given by the function $\Pi(\varphi) = \sin(\varphi + \beta)$, where β allows to control various modalities. For example, $\beta = \pi$ gives rise to an STDP-like plasticity rule, while $\beta = 3\pi/2$ qualitatively represents the Hebbian learning rule [32,33].

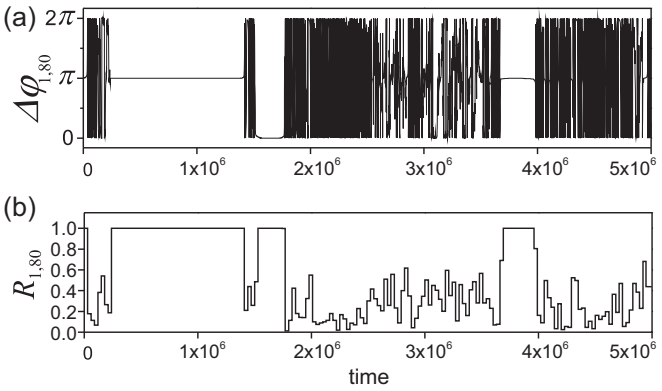

FIG. 2. The dynamics of a randomly chosen pair of oscillators. (a) The phase lag between the two oscillators $\Delta\varphi_{1,80} \equiv \varphi_1 - \varphi_{80} \bmod 2\pi$. (b) The transient degree of synchrony between the same oscillators. The network size $N = 200$, the parameters $\varepsilon = 0.01$, $\alpha = 1.4$, and $\beta = 4.94$.

III. RESULTS

For the rest of the paper, we use the parameter values $\varepsilon = 0.01$, $\alpha = 1.4$, and $\beta = 4.94$ unless otherwise is stated. We observe the dynamics of the network starting from random initial conditions. The initial phases are drawn from a uniform distribution $\varphi \in [0, 2\pi]$, the coupling coefficient from a uniform distribution $\kappa \in [-1, 1]$.

While observing the network collective dynamics, our attention was drawn by a peculiar regime which, to the best of our knowledge, has not been reported before. We first noticed this regime when we observed the temporal dynamics of phase lags between different oscillators. For certain parameters, these lags demonstrated intermittent behavior: The two oscillators alternated between the periods of phase locking and incoherence. This behavior is illustrated in Fig. 2(a) for a randomly selected pair of oscillators, and it is very similar for all other pairs.

In order to gain sight of a broader picture on the whole network scale, we calculated the transient degree of synchrony between the oscillators defined as follows:

$$R_{jk}(t) = \frac{1}{\Delta}\left|\int_t^{t+\Delta} e^{i[\varphi_j(t) - \varphi_k(t)]}dt\right|. \tag{3}$$

Here t is the current time and Δ is a (sufficiently large) time window. In order to capture the intermittent behavior described above, Δ must be much larger than the native period of the oscillators but much smaller than the typical duration of the coherence and incoherence episodes. Further, we usd $\Delta = 3000$, but the results do not significantly change for other values of Δ in a wide range. Figure 2(b) shows the evolution of the transient degree of synchrony between the two oscillators whose dynamics is depicted in Fig. 2(a). It is close to 1 while the phases of the two oscillators are locked and smaller than 1 while they drift apart.

We analyzed the degree of synchrony of all the oscillator pairs across the network depending on time. The resulting matrices R_jk are presented in Fig. 3 along with the snapshots of the phases and mean frequencies. The mean frequency of each oscillator was calculated along the time interval Δ. The

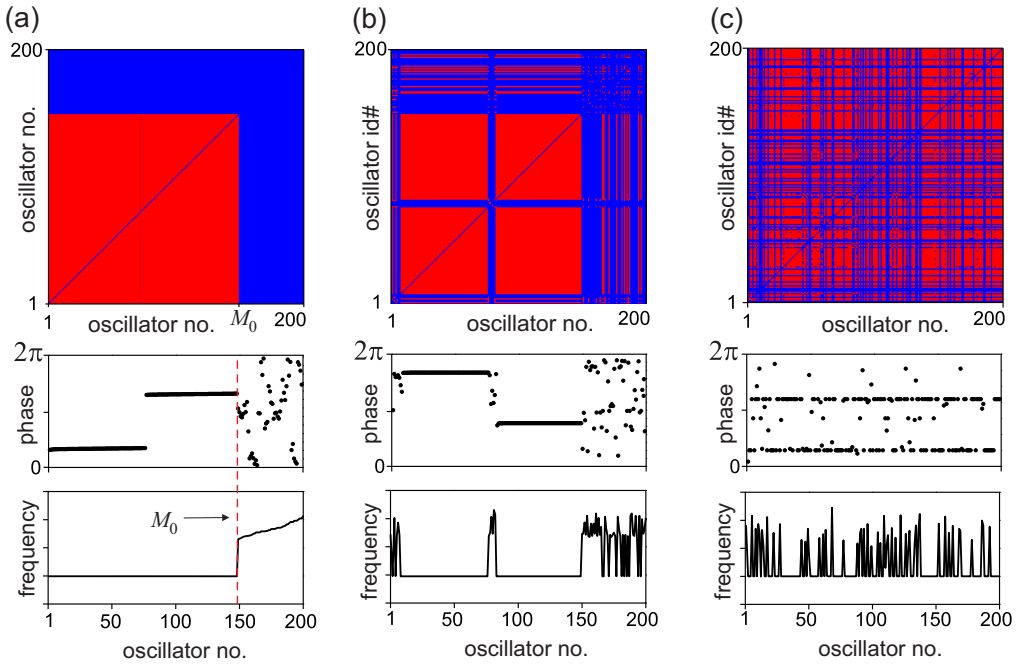

FIG. 3. The network states at subsequent time moments: (a) at $t = t_0 = 5 \times 10^5$, after the indexes renumbering; (b) at $t = t_1 = 6.5 \times 10^5$; (c) at $t = t_2 = 8.5 \times 10^5$. In the upper panels, the matrix of the transient degrees of synchrony R_{jk} is plotted. Red (light gray) corresponds to strong synchrony $R_{jk} > R^*$, where $R^* = 0.999$. Blue (dark gray) corresponds to weak synchrony $R_{jk} < R^*$. In the middle and bottom panels, the phases and the mean frequencies of the oscillators are presented. In (a), the core size M_0 is indicated by the red dashed line. The network size $N = 200$, the parameters $\varepsilon = 0.01$, $\alpha = 1.4$, and $\beta = 4.94$.

major finding is that the oscillators split into two domains. The first domain demonstrates strong synchronization which is manifested by the degree of synchrony close to 1. The oscillators of the second domain show low synchrony with those from the first domain and also between each other. In order to reveal this splitting we renumbered the oscillators according to their degree of synchrony at the particular time moment $t = t_0 = 5 \times 10^5$. Then, the coherent domain consists of the oscillators with indexes from 1 to M_0, and the incoherent one of the oscillators with indexes from $M_0 + 1$ to N, where $M_0 = 148$ is the size of the coherent domain at t_0. The state of the network with renumbered indexes is illustrated in Fig. 3(a). One sees that the coherent domain consists of two antiphase clusters, while the incoherent domain has a broad distribution of phases. The frequencies of the oscillators from the coherent domain are equal, while those of the incoherent domain are widely distributed. This frequency profile is typical for chimera states.

The splitting of the oscillators into the two domains, the coherent and the incoherent ones, strongly resembles a chimera state. However, there is a drastic difference between the classical chimeras and the regime that we observe. In order to trace it we fixed the oscillator indexes and observed the long-term evolution of the network. Then we noticed that the composition of the coherent and the incoherent domains was volatile, meaning that each particular oscillator spontaneously switched from one domain to another. In order to demonstrate this volatility we illustrate the network states in subsequent moments of time. In Fig. 3(b), the coherent and the incoherent domains are still present at $t = t_1 = 6.5 \times 10^5$, but their composition is different compared to $t = t_0$. The oscillators which constitute the domains are not longer ordered but rather mixed across the network. This mixing goes even further in Fig. 3(c) for $t = t_2 = 8.5 \times 10^5$.

To better picture the process of mixing of the coherent and the incoherent domains we studied the temporal evolution of their composition. At each time moment we calculated the transient degrees of synchrony and determined the domain attribute u_j of each oscillator. The oscillator was attributed belonging to the coherent domain with $u_j = 1$ if it was strongly synchronized with some others, and to the incoherent one with $u_j = 0$ if it has no strong synchrony with any others. The composition of the domains is plotted versus time in Fig. 4, with red (light gray) corresponding to the coherent and blue (dark gray) to the incoherent domain. At the time t_0 just after the oscillators renumbering the domains are ordered. As the time passes the oscillators spontaneously switch their domains. From the network viewpoint, this process corresponds

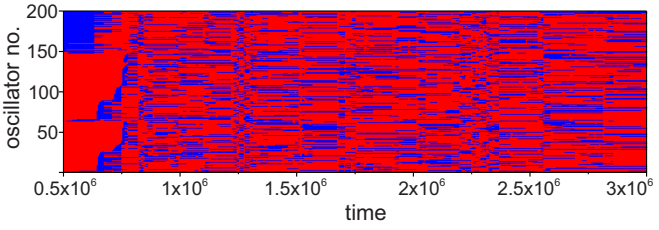

FIG. 4. The evolution of the coherent and incoherent domains of the coherent of the itinerant chimera. Red (light gray) corresponds to the coherent, blue (dark gray) to the incoherent domain. The network size $N = 200$, the parameters $\varepsilon = 0.01$, $\alpha = 1.4$, and $\beta = 4.94$.

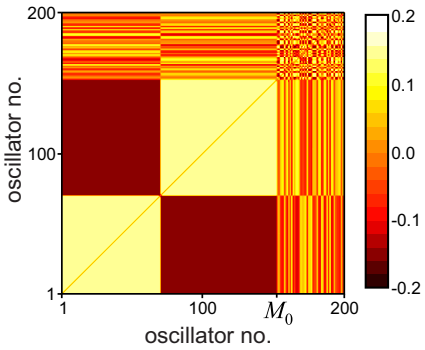

FIG. 5. Coupling matrix κ_{jk} at the moment $t = t_0$ after the oscillators renumbering. The network size $N = 200$, the parameters $\varepsilon = 0.01$, $\alpha = 1.4$, and $\beta = 4.94$.

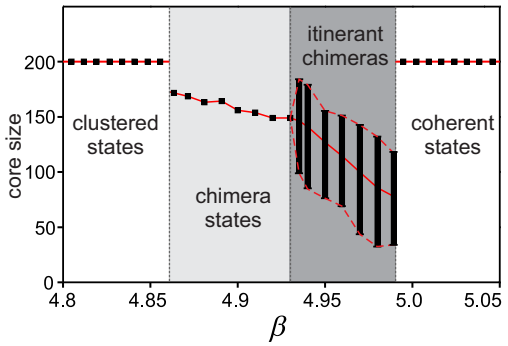

FIG. 6. Core size versus the parameter β. Black bars denote the points where the simulations were performed. For itinerant chimeras, the mean core size is plotted by a solid line and minimal and maximal values by dashed lines. The network size $N = 200$, the resting parameters $\varepsilon = 0.01$, $\alpha = 1.4$.

to the volatility of the domains composition. The coherent domain, which is often called the chimera's core, does not stay in the same position but rather moves spontaneously across the network. This feature led us to adopt the name "itinerant chimera" to the observed regime.

The splitting of the oscillators into two domains is supported by the sufficient structure of the coupling matrix which is depicted in Fig. 5 for $t = t_0$. Note that this moment corresponds to the network state illustrated in Fig. 2(a) when the oscillator indexes are renumbered so that the coherent domain consists of oscillators $1, \ldots, M_0$, and the incoherent domain of oscillators $M_0 + 1, \ldots, N$. Recall that the coherent domain consists of two antiphase clusters. The oscillators within each synchronous cluster have strong positive connections, while the two clusters have strong negative connections between each other. These strong and structured connections are the reason for the synchrony within the coherent domain. At the same time, the connections within the incoherent domain and between the two domains do not show any structure; they may be either negative or positive as well as strong or weak. This diversity determines the lack of synchrony within the incoherent domain. Note that the structure of the coupling matrix is not prescribed but rather emerges from the random initial conditions due to the network adaptivity. During the further network evolution when the core composition changes, the coupling matrix changes as well, but its basic features remain: The connections within the core are strong and well structured, while the resting connections do not show any structure.

The itinerant chimeras are robust patterns which persist under the variation of the system parameters. In order to prove that we changed the parameters α, β, and ε and analyzed the observed behavior patterns. The results are presented in Fig. 6 where the core size M is plotted versus the parameter β (the data for other parameters variation is not shown). The core size is calculated as the number of the synchronized oscillators $M = \sum_j u_j$. For $\beta < 4.86$ the oscillators split into several clusters of synchrony, therefore the "core" occupies the whole network and $M = N$. For $4.86 < \beta < 4.93$ classical chimeras are observed for which the composition and the size of the core do not change with time. The itinerant chimeras are observed for $4.93 < \beta < 4.99$, and in this parameter interval not only the constitution but also the size of the core changes with time. For $\beta > 4.99$ the system undergoes a transition to the coherent state.

Further, we investigate in more detail the traveling of the core and demonstrate that it is not only a finite-size effect but rather a keynote feature of the network dynamics which is preserved even for a large number of nodes. The dynamics of the core size is illustrated in Fig. 7(a); it demonstrates pronounced fluctuations around the mean. The size fluctuations suggest randomlike transitions of the oscillators between the domains. These transitions appear to be positively correlated meaning that the oscillators tend to switch their domain in groups. In order to illustrate that we plot the distribution of the chimera core size M observed in a long time interval in Fig. 7(b). For the independent randomlike switching of individual oscillators the core size would have binomial distribution $M \sim B(N, p)$, where p is the fraction of the oscillators belonging to the core. However, the obtained distribution is

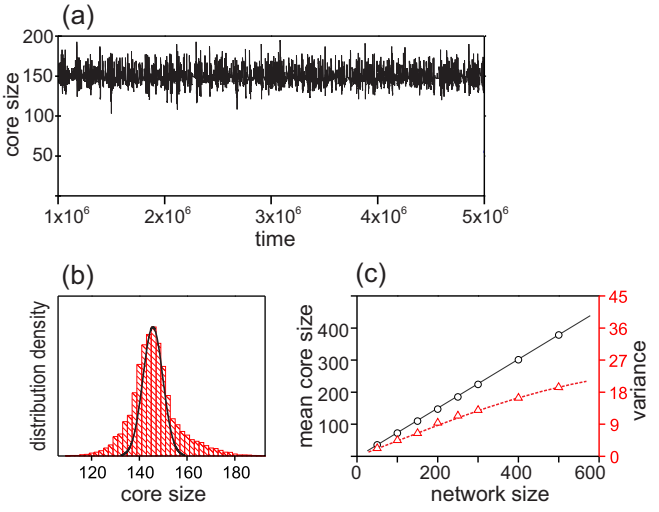

FIG. 7. (a) The chimera core size versus time for $N = 200$. (b) Distribution of the core size for $N = 200$. Black solid line corresponds to the binomial distribution. (c) The mean (black solid line) and the variance (red dashed line) of the core size versus the network size. The parameters $\varepsilon = 0.01$, $\alpha = 1.4$, and $\beta = 4.94$.

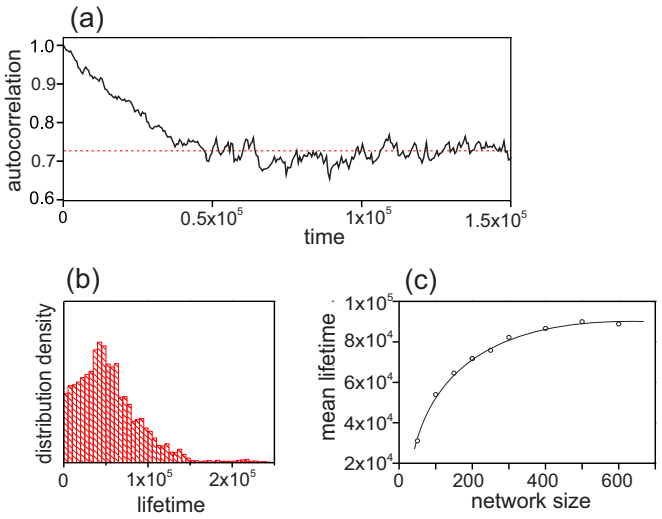

FIG. 8. (a) Autocorrelation function of the core composition versus time for $N = 200$. The horizontal dashed line corresponds to $A = p$. (b) Distribution of the nodes lifetimes in the core for $N = 200$. (c) The mean lifetime versus the network size. The parameters $\varepsilon = 0.01$, $\alpha = 1.4$, and $\beta = 4.94$.

much wider and has much heavier tails, suggesting concurrent transitions of large groups of oscillators.

In order to study the scaling of the itinerant chimeras we plot the mean and the variance of the core size M versus the network size N in Fig. 7(c). The mean core size $\langle M \rangle$ grows linearly with the network size suggesting the constant ratio between the coherent and the incoherent domains. The fraction of the oscillators in the core may be estimated as $p = \langle M \rangle / N \approx 0.72$. The variance $\sigma_M = \sqrt{\langle M^2 \rangle - \langle M \rangle^2}$ grows sublinearly; however, it is much larger than that predicted by the binomial distribution. The wide distribution of the core size corroborates that the core volatility manifests itself on the macroscopic level, not only as a finite-size effect.

To prove the randomlike character of the oscillators switching between the domains, we introduce the autocorrelation function of the core composition defined as

$$A(\tau) = \frac{1}{\langle M \rangle} \lim_{t \to \infty} \frac{1}{T} \int_0^T \sum_{j=1}^{N} u_j(t) u_j(t+\tau) dt. \qquad (4)$$

Here the sum under the integral is nothing but the number of the oscillators which belong to the core at the both time moments t and $t + \tau$. The function $A(\tau)$ gives the mean fraction of the oscillators which stay in the core (or return back to it) in time τ. The autocorrelation function $A(\tau)$ is plotted in Fig. 8(a). It equals unity at $\tau = 0$ and falls to $A \approx p$ at $\tau \sim 5 \times 10^4$, which corresponds to the fraction of units shared by two randomly selected sets. This means that the network memory about the core composition fades completely in this time, the core effectively spreads across the network, and its composition becomes unpredictable. The correlation decay is a clear sign of the chaotic dynamics, which we confirmed by the calculation of the largest Lyapunov exponent $\lambda = 0.0045$. Note, however, that the inverse time $\lambda^{-1} = 222$ is much shorter than the typical time of the core spreading.

Another way to estimate the rate of the core traveling is to compute the lifetimes of individual oscillators in the core. The distribution of the lifetimes is shown in Fig. 8(b); it is a broad unimodal distribution with an average of about 5×10^4, which roughly corresponds to the result from Fig. 8(a). The scaling behavior of the mean lifetime is illustrated in Fig. 8(c). Although the lifetime grows with the network size, this growth is relatively slow and tends to saturate, in sharp contrast with the lifetime of classic chimeras, which was shown to increase exponentially [9]. Thus, the finite-speed traveling is preserved even for large networks.

IV. CONCLUSIONS

We have studied a new type of chimera-like behavior observed in networks of oscillators with adaptive coupling. Similarly with classical chimeras, the oscillators split into two domains, coherent and the incoherent. However, the drastic difference is that the composition of the coherent and incoherent domains changes with time. The oscillators spontaneously switch their domain, which results in traveling of the chimera's core across the network. This process is characterized by fading memory, meaning that the network forgets the composition of the core in a finite time. The lifetime of the core grows slowly with the network size, suggesting that the core volatility is not a finite-size effect but rather an intrinsic feature of the network collective dynamics.

Our system may also demonstrate other collective behaviors depending on the parameters α and β. In particular, we observed classical chimera states and the emergence of clustered states similar to those described earlier for continuous coupling [34]. However, we conjecture that the pulse nature of coupling together with its adaptivity was crucial for the emergence of itinerant chimeras. Provided that the major motivation for the model comes from neuroscience, it would be intriguing to search for similar dynamical regimes in biologically plausible setups and explore their possible role in collective dynamics of neuronal populations.

ACKNOWLEDGMENTS

The authors are grateful to Anna Zakharova and Christian Bick for many helpful discussions. The work was supported by the Russian Foundation for Basic Research (Projects No. 17-02-00904, No. 17-02-00874, No. 18-02-00406, and No. 18-29-10040).

[1] S. Boccaletti, V. Latora, Y. Moreno, M. Chavez, and D.-U. Hwang, Phys. Rep. **424**, 175 (2006).
[2] Y. Kuramoto and D. Battogtokh, Nonlin. Phenom. Complex Syst. **5**, 380 (2002).
[3] D. M. Abrams and S. H. Strogatz, Phys. Rev. Lett. **93**, 174102 (2004).
[4] M. J. Panaggio and D. M. Abrams, Nonlinearity **28**, R67 (2015).
[5] O. E. Omelchenko, Nonlinearity **31**, R121 (2018).

[6] D. M. Abrams, R. Mirollo, S. H. Strogatz, and D. A. Wiley, Phys. Rev. Lett. **101**, 084103 (2008).
[7] M. Wolfrum, O. E. Omelchenko, S. Yanchuk, and Y. Maistrenko, Chaos **21**, 013112 (2011).
[8] O. E. Omelchenko, Nonlinearity **26**, 2469 (2013).
[9] M. Wolfrum and O. E. Omelchenko, Phys. Rev. E **84**, 015201 (2011).
[10] O. E. Omelchenko, M. Wolfrum, and Y. L. Maistrenko, Phys. Rev. E **81**, 065201 (2010).
[11] W. Dednam, M. J. Caturla, and A. E. Botha, Europhys. Lett **123**, 60004 (2018).
[12] D. P. Rosin, D. Rontani, N. D. Haynes, E. Schöll, and D. J. Gauthier, Phys. Rev. E **90**, 030902(R) (2014).
[13] M. Shanahan, Chaos **20**, 013108 (2010).
[14] S. W. Haugland, L. Schmidt, and K. Krischer, Sci. Rep. **5**, 9883 (2015).
[15] R. Ma, J. Wang, and Z. Liu, Europhys. Lett. **91**, 40006 (2010).
[16] C. Bick, Phys. Rev. E **97**, 050201(R) (2018).
[17] J. Xie, E. Knobloch, and H.-C. Kao, Phys. Rev. E **90**, 022919 (2014).
[18] C. Bick (private communication).
[19] B. K. Bera, D. Ghosh, and T. Banerjee, Phys. Rev. E **94**, 012215 (2016).
[20] A. Mishra, S. Saha, D. Ghosh, G. V. Osipov, and S. K. Dana, Opera Med. Physiol. **3**, 14 (2017).
[21] J. Sawicki, I. Omelchenko, A. Zakharova, and E. Schöll, Euro. Phys. J. Spec. Top. **226**, 1883 (2017).
[22] C. Bick and E. A. Martens, New J. Phys. **17**, 033030 (2015).
[23] I. Omelchenko, O. E. Omel'chenko, A. Zakharova, M. Wolfrum, and E. Schöll, Phys. Rev. Lett. **116**, 114101 (2016).
[24] I. Omelchenko, O. E. Omel'chenko, A. Zakharova, and E. Schöll, Phys. Rev. E **97**, 012216 (2018).
[25] V. V. Klinshov and V. I. Nekorkin, Chaos **27**, 101105 (2017).
[26] J. Rinzel and G. B. Ermentrout, in *Methods in Neuronal Modeling: From Synapses to Networks*, edited by C. Koch and I. Segev (MIT Press, Cambridge, 1998), Vol. 2, pp. 251–291.
[27] S. Achuthan and C. C. Canavier, J. Neurosci. **29**, 5218 (2009).
[28] W. Gerstner, R. Kempter, J. L. van Hemmen, and H. Wagner, Nature **383**, 76 (1996).
[29] A. Morrison, M. Diesmann, and W. Gerstner, Biol. Cybern. **98**, 459 (2008).
[30] M. Gilson, A. N. Burkitt, and J. L. van Hemmen, Front. Comput. Neurosci. **4**, 23 (2010).
[31] Note that the matrix κ_{jk} encodes both the weights and topology of the connections: even if we start from all-to-all coupling, in principle some connections may weaken with time and extinct due to the plasticity. Note also that we do not allow for self-coupling.
[32] T. Aoki and T. Aoyagi, Phys. Rev. Lett. **102**, 034101 (2009).
[33] T. Aoki and T. Aoyagi, Phys. Rev. E **84**, 066109 (2011).
[34] D. V. Kasatkin, S. Yanchuk, E. Schöll, and V. I. Nekorkin, Phys. Rev. E **96**, 062211 (2017).